Kinetic Energy Release Distribution in the Dissociation of Toluene Molecular Ion. The Tropylium vs Benzylium Story Continues

Jeong Hee Moon,[†] Joong Chul Choe,[‡] and Myung Soo Kim*,[†]

National Creative Research Initiative Center for Control of Reaction Dynamics and Department of Chemistry, Seoul National University, Seoul 151-742, Korea, and Department of Chemistry, University of Suwon, Suwon 440-600, Korea
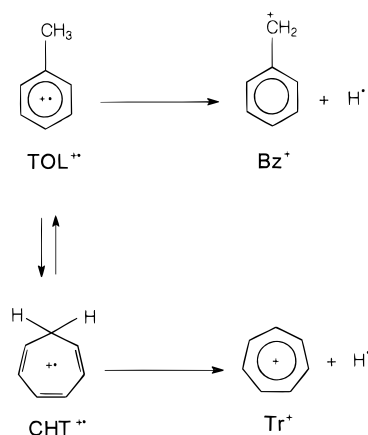
Production of $C_7H_7^+$ from toluene molecular ion (TOL$^{•+}$) was studied using mass-analyzed ion kinetic energy spectrometry. The kinetic energy release distribution (KERD) was determined, which showed that both benzylium (Bz$^+$) and tropylium (Tr$^+$) ions were produced from TOL$^{•+}$. The interconversion between the molecular ions of toluene and cycloheptatriene prior to the dissociations was confirmed. Ab initio calculations at the HF/6-31G** and G2(MP2,SVP) levels were carried out for some important chemical species. The KERD in the Bz$^+$ channel was calculated using the statistical phase space theory, while classical trajectory calculations were done to obtain the theoretical KERD in the Tr$^+$ channel. The Tr$^+$/Bz$^+$ branching ratio determined by analyzing the experimental KERD was much larger than reported previously.

Introduction

Production of $C_7H_7^+$ from toluene molecular ion (TOL$^{•+}$) is one of the most extensively studied reactions in the field of gas-phase ion chemistry.[1–13] Investigations over the years have established that two isomeric ions, namely, benzylium (Bz$^+$) and tropylium (Tr$^+$), are produced, the former by a simple C−H bond cleavage of TOL$^{•+}$ and the latter via isomerization to the cycloheptatriene (CHT$^{•+}$) structure and subsequent C−H bond cleavage (Scheme 1).

Since the enthalpy of formation of Tr$^+$ is lower than that of Bz$^+$ (by ∼0.4 eV), one would expect the preferential generation of Tr$^+$ near the threshold for the dissociation of TOL$^{•+}$. Dunbar[3] measured the Tr$^+$/Bz$^+$ branching ratio using the ion cyclotron resonance (ICR) technique based on the hypothesis[2] that only Bz$^+$ reacts with toluene to produce $C_8H_9^+$. It was found that the Bz$^+$ channel competed effectively against the Tr$^+$ channel even very near the reaction threshold. The same was observed in the time-resolved photoionization study of Lifshitz and co-workers, which also utilized the Bz$^+$−toluene reaction.[6–8] Moreover, it was found that the appearance energies for Bz$^+$ and Tr$^+$ were essentially the same, which is in agreement with the effective competition between the two channels observed even very near the threshold. However, this is in apparent contradiction with the fact that Tr$^+$ is more stable than Bz$^+$.[14] The issue was more or less resolved by the quantum chemical study of Lifshitz and co-workers, which found that a substantial (∼0.4 eV) reverse barrier was present in the dissociation of CHT$^{•+}$ to Tr$^+$ and that the height of the TOL$^{•+}$ → CHT$^{•+}$ barrier was lower than those for the dissociation to Bz$^+$ and Tr$^+$.[7] Another important result for this system is the accurate rate−energy relation for the overall reaction, namely, Bz$^+$ plus Tr$^+$, determined by Huang and Dunbar with the time-resolved photodissociation technique.[13] The tropylium vs benzylium story has been reviewed by Lifshitz recently.[1]

* To whom correspondence should be addressed.
† Seoul National University.
‡ University of Suwon.

SCHEME 1

The previous investigations on this system described above were focused mainly on the branching ratios and the rate constants. No serious study on the exit channel effect has been made for this system, even though a successful mechanistic model should be compatible not only with the rate−energy and branching ratio data but also with the exit channel data.[15–27] Practically the most important exit channel information in gas-phase ion chemistry is the kinetic energy release distribution (KERD), which can be measured easily and accurately. Various information on a reaction is available from the measured KERD such as the presence of the reverse barrier. In some cases, KERD appears as bimodal due to the production of two isomeric products. Then, it is possible to separate KERD into components and determine their branching ratio.[24,25] Also, it is possible to calculate KERD with statistical or dynamical theories and compare the results with the experimental data so as to gain further insights into the process.

In this work, a combined experimental and computational study on KERD in the metastable decomposition of TOL$^{•+}$ is presented. It will be shown that the previous mechanistic model is compatible with the present KERD data and that a further

improvement in kinetic modeling is needed for a quantitative explanation of the process.

Experimental Section

A double-focusing mass spectrometer with reversed geometry (VG ZAB-E) was used. Toluene or cycloheptatriene was introduced to the ion source via a septum inlet and was ionized by 70 eV electron ionization. The ion source temperature was maintained at 180 °C, and ions generated were accelerated to 8 keV. Mass-analyzed ion kinetic energy spectrometry (MIKES) was used to observe the unimolecular dissociation of TOL•+. Namely, the molecular ion was separated by the magnetic sector, and the translational kinetic energy of a product ion generated in the second field-free region of the instrument was analyzed by the electric sector. To improve the quality of a MIKE spectrum, signal averaging was carried out for repetitive scans. The MIKE profile of $C_7H_7^+$ was recorded with an energy resolution higher than 8000 measured at half-height. Under this condition, deconvolution of the instrumental broadening was not needed in the calculation of KERD from the MIKE profile because the main beam bandwidth was negligible compared to that of $C_7H_7^+$.

Calculations

Ab Initio Calculation. The ab initio molecular orbital calculations were performed for the optimized geometries of some important species at the levels of HF/6-31G** and G2-(MP2,SVP)[28,29] using the GAUSSIAN 94[30] suite of programs on a CRAY-T3E computer. These include TOL•+, CHT•+, Bz+, Tr+, and the transition state (TS(Tr)) for CHT•+ → Tr+ + H•. The potential energies at the G2(MP2,SVP) level for Bz+ and Tr+ are in agreement with the previous values,[31] while this is the first report of the TOL•+, CHT•+, and TS(Tr) energies at the G2(MP2,SVP) level. The zero-point energies of these species at the HF/6-31G** level were calculated using the vibrational frequencies scaled by 0.90.

Statistical Calculation of KERD in the Bz+ Channel. The statistical phase space theory was used to calculate the KERD in the simple bond cleavage of TOL•+ to Bz+ + H•.[18]

$$n(T;J,E) \propto \int_{R_m}^{E-E_0-T} \rho(E-E_0-T-R)\, P(T,J,R)\, \mathrm{d}R \quad (1)$$

Here, $n(T;J,E)$ is the KERD at the angular momentum J and the internal energy E. The root-mean-square average J evaluated at the ion source temperature was used. ρ and P are the product vibrational and angular momentum state densities, respectively. R is the product rotational energy and R_m is its minimum. E_0 is the reaction critical energy. Applicability of the phase space theory in the H•-loss reaction will be discussed later.

Classical Trajectory Calculation of KERD in the Tr+ Channel. Details of the classical trajectory method modified in this laboratory to study the dissociation of polyatomic molecules have been reported already.[16] Only a brief summary of the overall procedure will be described here together with the details of the modification made for the present study.

The potential energy surface (PES) for the CHT•+ → Tr+ + H• reaction was constructed by interpolation of local harmonic potentials obtained by ab initio calculations. Since the computation of the energy, gradient, and Hessian was very time-consuming, ab initio calculation was limited to the HF/6-31G** level (3 h/point with CRAY-T3E). In addition to the computational economy, the fact that the relative potential energies of the major species calculated at the HF/6-31G** and G2-

(MP2,SVP) levels are comparable (to be shown) led us to adopt the HF/6-31G** level for the dynamical study. In our previous trajectory studies, local potentials at some (usually 40) points along the intrinsic reaction coordinate (IRC) and more at off-IRC points (usually 300) were used to construct the PES. In the present case, we had to be content with the PES constructed with the local potentials at the 40 IRC points only due to the tremendous computational demand. This, the IRC-only PES, is a good approximate PES as far as the exit channel trajectories do not deviate too much from the IRC, which is likely for the present reaction which proceeds via a rather simple extension of a C−H bond.

In our previous studies, the initial conditions for the trajectory calculations were sampled according to the orthant-like sampling scheme in which the momentum was sampled randomly with the molecular geometry fixed at the saddle point.[15,16] We had tremendous difficulties with this approach in the present case, however. In particular, the seven-membered carbon ring, which remains planar along the IRC, was found to be severely distorted in most of the configurations along the trajectories. Namely, trajectories probed regions in the configuration space which were far off from the IRC and where the IRC-only PES was not reliable. This arose, we found, because the orthant-like sampling supplied too much energy in the low-frequency ring modes, corresponding to several quanta even when only the total zero-point energy at the saddle point was distributed. To avoid this problem, we devised a simple and more realistic scheme which may be called the geometry-fixed normal mode sampling. Here, the geometry was fixed at the saddle point as before, and each mode was assigned with its own zero-point energy. Then, the average thermal energy (ϵ_i) in each mode expected at the given quantum mechanical excess energy (E_{ex}) at the TS, namely, the energy above the zero-point level of the saddle point, was calculated and added to the above zero-point energy.

$$E_{ex} = (1/2)k_B T^* + \sum \epsilon_i \quad (2)$$

with

$$\epsilon_i = \frac{h\nu_i}{\exp(h\nu_i/k_B T^*) - 1} \quad (3)$$

In eq 2, the first term is the average kinetic energy for the 1-dimensional translation along the reaction path. ν_i and T^* are the vibrational frequencies and the effective temperature at the TS. With the mode energy fixed, the magnitude of the momentum vector is also fixed. Hence, two different momentum states are possible for each mode depending on its phase, forward or backward. For the 15-atom system ($3N - 6 = 39$), the total number of momentum states becomes 2^{39}. In the present work, the initial condition was selected randomly among these states. With this scheme, the ring distortion along the trajectory was much reduced.

A total of 3000 trajectories were calculated. Each trajectory was integrated using the fourth-order Runge−Kutta (RK4) method[32] with a time step of 0.05 fs. The energy conservation error was less than 10^{-7} throughout the integration.

Results and Discussion

The schematic potential energy diagram for the two dissociation pathways is shown in Figure 1. The energies of some important structures calculated at the G2(MP2,SVP) level are indicated in the figure, which do not differ too much from the corresponding values obtained at the HF/6-31G** level. We
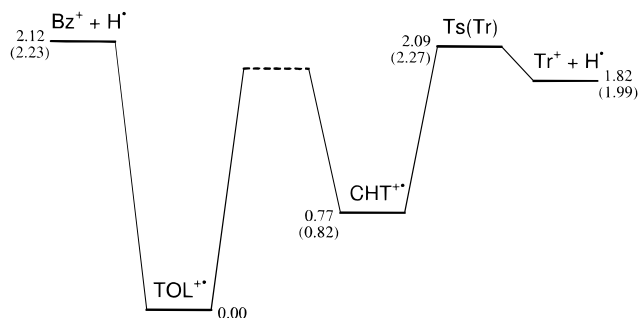
Figure 1. Schematic potential energy diagram for the production of Bz^+ and Tr^+ from $TOL^{\bullet+}$. The isomerization barrier between $TOL^{\bullet+}$ and $CHT^{\bullet+}$ has not been calculated. An arbitrary level is drawn taking into account the results in ref 7. The numbers denote the potential energies (eV) at the vibrational zero points obtained at the G2(MP2,-SVP) level and referred to that of $TOL^{\bullet+}$. The numbers in parentheses are energies calculated at the HF/6-31G** level.
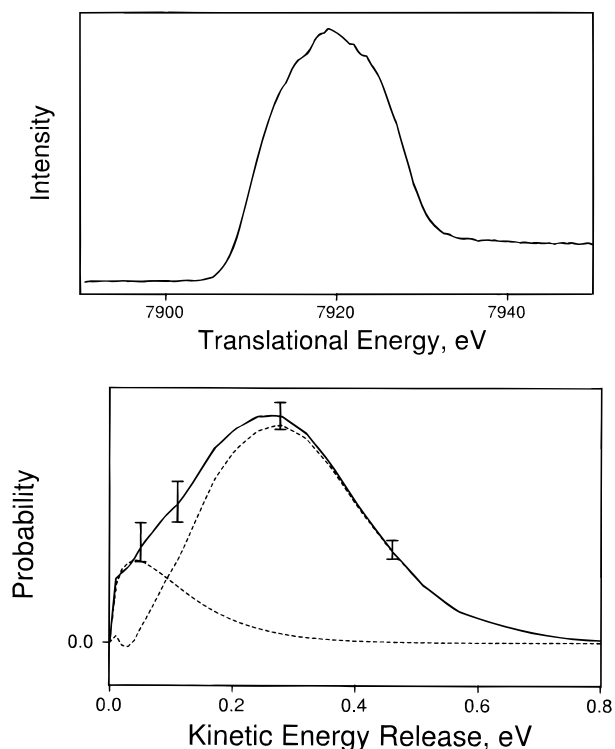

Figure 2. (a, top) MIKE profile of $C_7H_7^+$ produced by unimolecular dissociation of $C_7H_8^{\bullet+}$ generated by electron ionization of toluene. (b, bottom) The solid curve represents the experimental KERD evaluated from the profile in (a). This has been separated into two components (dashed curves), Bz^+ and Tr^+, assuming 15% Bz^+ contribution. The curve with smaller kinetic energy release is the Bz^+ component. Experimental error limits are shown (I). See the text for details.

could not determine the complete pathway between $TOL^{\bullet+}$ and $CHT^{\bullet+}$ at the ab initio levels adopted in this work. We will just mention that there is a general consensus among investigators that the barrier height for the isomerization is lower than those for the dissociations.

Production of $C_7H_7^+$ was the only channel in the unimolecular decay of $C_7H_8^{\bullet+}$ generated by electron ionization of toluene. Its MIKE profile is shown in Figure 2a. The continuum background on the high-energy side of the peak is due to the dissociation occurring inside the electric sector. The low-energy half of the peak was used to evaluate KERD according to the method of Yeh and Kim.[33] It is well-known that a small kinetic energy release in the center-of-mass (COM) frame results in a large spread in the laboratory energy.[34] This COM-to-laboratory

magnification of KER is rather small for $H^{\bullet}$ loss because of the small neutral mass. To see if the above analytic method to evaluate KERD was valid in this extreme case also, the analytic basis function, namely, the MIKE profile at a single KER, was compared with the exact profile calculated using the third-order ion optics (TRIO) program developed by Matsuo et al.[35] The two profiles were essentially identical, confirming the validity of the analytic approach. KERD evaluated from the MIKE profile in Figure 2a is shown in Figure 2b. The MIKE profile for the $H^{\bullet}$ loss from $CHT^{\bullet+}$ was recorded, and KERD was evaluated also. KERDs for the $H^{\bullet}$ losses from $TOL^{\bullet+}$ and $CHT^{\bullet+}$ (not shown) are identical, in agreement with the rapid inter-conversion between these structures as postulated in Scheme 1. The shape of the KERD looks rather peculiar when compared to those for other reactions reported previously.[15-27] It looks as if the overall KERD consists of more than one component even though the bimodality is not clear. In the following, an attempt will be made to understand this peculiar KERD pattern by comparison with the theoretical results.

As is well accepted,[1] $TOL^{\bullet+} \rightarrow Bz^+ + H^{\bullet}$ is most likely a simple bond cleavage without a noticeable reverse barrier.[36] It is also well-known that the statistical phase space theory provides a rather accurate prediction for KERD in such a simple bond cleavage reaction.[18,25-27] Recently, Lifshitz suggested that KERs for the $H^{\bullet}$ loss could be much greater than expected from the phase space theory,[37] citing the works of Bersohn and co-workers[38] and Bowers and co-workers.[39] We will not go into details of Bersohn and co-workers' work because KER was not calculated by the phase space theory in that work. We will just mention that the KER for the $H^{\bullet}$ loss larger than thermally expected arises from the significant dynamical effect associated with the small hydrogen mass, which is partially accounted for in the phase space theory. In the case of $C_4H_8^{\bullet+} \rightarrow C_4H_7^+ + H^{\bullet}$ investigated by Bowers and co-workers, the presence of a small reverse barrier has been reported,[40] and hence the validity of the phase space theory calculation of KERD cannot be tested with this system.[41] As a test of the phase space theory in the $H^{\bullet}$ loss, we have measured and calculated the KERD for $C_6H_6^{\bullet+} \rightarrow C_6H_5^+ + H^{\bullet}$ and found a decent agreement between experiment and theory.[42] Also, we have found that a proper treatment of the instrumental broadening or recording of a MIKE profile at high-energy resolution is essential to obtain an accurate KERD in the case of the $H^{\bullet}$ loss reaction.

The molecular parameters used in the phase space theory calculation of the KERD in $TOL^{\bullet+} \rightarrow Bz^+ + H^{\bullet}$ are listed in Table 1. The critical energy of 2.23 eV obtained by ab initio calculation at the HF/6-31G** level was adopted. This was because the classical trajectory calculation for $CHT^{\bullet+} \rightarrow Tr^+ + H^{\bullet}$ to be presented later was done with PES constructed at the HF level also. The internal energy distribution of $TOL^{\bullet+}$ undergoing dissociation in the second field-free region of the instrument was estimated from the random lifetime distribution: $P(E) \propto \exp[-k(E)\tau_1] - \exp[-k(E)\tau_2]$. Here, $k(E)$ is the rate–energy relation. τ_1 and τ_2 are the transit times of $TOL^{\bullet+}$ to the entrance and exit of the second field-free region, which are 16 and 29 μs, respectively. The rate–energy relation reported by Huang and Dunbar was utilized.[13] The average internal energy of the dissociating $TOL^{\bullet+}$ thus determined was 3.31 eV. The KERD calculated at this internal energy is shown in Figure 3. Use of the internal energy distribution rather than the average internal energy resulted in essentially the same KERD. As far as the reaction proceeds statistically, the KERD in Figure 3 is expected to be correct within 20% in terms of the average kinetic energy release according to our experience.[26,27] Comparing the

TABLE 1: Molecular Parameters Used in the Phase Space Theory Calculation of KERD in TOL$^{\bullet+}$→ Bz$^+$ + H$^{\bullet}$

	vibrational frequencies (cm^{-1})^a													
C$_7$H$_7^+$ (Bz$^+$)	3091	3063	3060	3041	3039	3034	2998	1595	1559	1552	1463			
	1431	1336	1321	1318	1166	1143	1120	1097	1054	1020	1008			
	983	971	953	849	788	784	633	616	587	514	410	345	340	164

	rotational constants (cm^{-1})^b			polarizability (10^{-24} cm^3)^c
C$_7$H$_8^{\bullet+}$ (TOL$^{\bullet+}$)	0.177	0.0862	0.0586	
C$_7$H$_7^+$ (Bz$^+$)	0.179	0.0945	0.0620	
H$^{\bullet}$				0.667

^{a} The HF/6-31G** results multiplied by 0.90. ^{b} The HF/6-31G** results. ^{c} Reference 43.

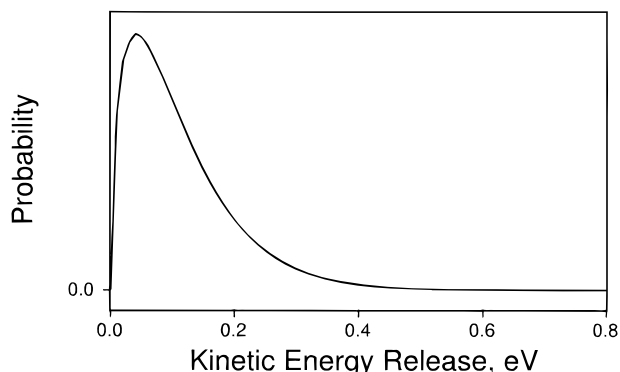**Figure 3.** KERD in TOL$^{\bullet+}$ → Bz$^+$ + H$^{\bullet}$ calculated with the phase space theory. See the text for details.

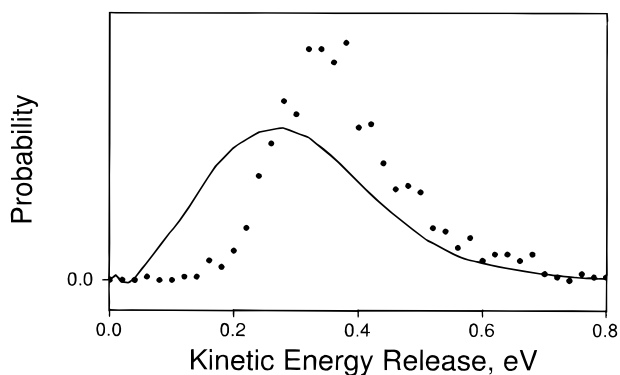**Figure 4.** The solid curve is the KERD in CHT$^{\bullet+}$→ Tr$^+$ + H$^{\bullet}$ estimated from the experimental data (Figure 2b) by subtracting 15% Bz$^+$ contribution. Circles denote the KERD obtained by the classical trajectory calculation.

KERDs in Figures 2b and 3, it is obvious that the experimental KERD cannot be explained at all with the TOL$^{\bullet+}$ → Bz$^+$ + H$^{\bullet}$ reaction alone.

The phase space theory is not adequate to evaluate the KERD in the CHT$^{\bullet+}$ → Tr$^+$ + H$^{\bullet}$ reaction because of the presence of the reverse barrier and the dynamical effect during the exit channel motion. Hence, the KERD for this reaction was evaluated by the classical trajectory calculation described in the previous section. The average internal energy of 3.31 eV for the dissociating TOL$^{\bullet+}$ corresponds to the average quantum mechanical excess energy of 1.04 eV at the saddle point. The KERD obtained by the classical trajectory calculation at this excess energy is shown in Figure 4. In our previous study of CH$_2$OH$^+$ → CHO$^+$ + H$_2$,[15] the KERD obtained by classical trajectory calculation was in good qualitative agreement, even though the fit was not quantitative. There are several reasons for the mismatch between the experimental and calculated results, the most obvious being the inaccuracy of the PES adopted in the calculation. This is likely to be even more serious

in the present case because the IRC-only local potentials were used to construct the PES. Regardless, it is gratifying to note in Figure 4 that the KERD calculated for CHT$^{\bullet+}$ → Tr$^+$ + H$^{\bullet}$ displays a large kinetic energy release, in agreement with previous reports on the production of Tr$^+$ from various precursor ions.[24,25] In particular, it is to be noted that the probability for small energy release (<0.2 eV) is negligible. This is expected for a reaction such as the present one in which the reaction coordinate overlaps substantially with the fragment separation coordinate.[44] Comparing Figures 2b and 4, it is obvious that the experimental KERD cannot be explained with the CHT$^{\bullet+}$ → Tr$^+$ + H$^{\bullet}$ channel alone. Rather, it looks likely that the experimental KERD consists of two components, TOL$^{\bullet+}$ → Bz$^+$ + H$^{\bullet}$ contributing to the lower and CHT$^{\bullet+}$ → Tr$^+$ + H$^{\bullet}$ to the higher energy parts. This is in agreement with the mechanistic model which is widely accepted at the moment.

Since the experimental KERD does not look bimodal, it is difficult to separate it into components using techniques such as the surprisal analysis.[25] The method adopted in this work is as follows. It was assumed that the KERD in the TOL$^{\bullet+}$ → Bz$^+$ + H$^{\bullet}$ reaction is well represented by the phase space theory calculation. Assuming that this channel contributes a certain fraction, say 10%, to the overall reaction, its contribution was subtracted from the experimental KERD. Particular attention was paid to the low-energy (<0.2 eV) portion of the remainder, which is presumably the KERD of the Tr$^+$ channel. An excessive subtraction resulted in negative probability in this portion, while an insufficient subtraction led to a bimodal-looking KERD for the Tr$^+$ channel. A successful separation with 15% Bz$^+$ contribution is shown in Figure 2b. KERD for the Tr$^+$ channel thus obtained is compared with that from the classical trajectory calculation in Figure 4. These two are in decent qualitative agreement. A much better fit is not expected as mentioned above. Varying the Bz$^+$ contribution in the above process, the range of the Tr$^+$/Bz$^+$ branching ratio resulting in the reasonable, namely, not unphysical, separation could be determined. The separation was also attempted with the theoretical KERDs for the Bz$^+$ channel whose average kinetic energy release was larger than that in Figure 3 by as much as 50%. Such theoretical KERDs was obtained by PST calculation with internal energies larger than 3.31 eV. The Tr$^+$/Bz$^+$ branching ratio thus estimated is 5 ± 2.

Dunbar determined the Tr$^+$/Bz$^+$ branching ratio by photodissociation in the ion cyclotron resonance spectrometer. Lifshitz carried out the Rice−Ramsperger−Kassel−Marcus (RRKM)[45] rate−energy calculation using ab initio energy and vibrational frequency data.[1,7] An excellent fit between the experimental and calculated branching ratios was reported. According to these data, the branching ratio of ∼1 is expected for the present unimolecular reaction occurring at the internal energy of 3.31 eV, in contrast with 5 ± 2 estimated in this work. We do not claim that the method used in this work is rigorous enough to

obtain an accurate branching ratio. However, the experimental and calculated KERDs in Figures 2b, 3, and 4 suggest that the equal contributions from the Bz^+ and Tr^+ channels are not likely. One can think of various explanations for the above discrepancy. One is to suppose that the kinetic energy release in the Bz^+ channel is larger than predicted by the phase space theory as suggested by Lifshitz for the $H^\bullet$ loss reactions. A systematic investigation for many simple C–H cleavage reactions would be useful in this regard. Another is to suppose that the chemical titration of Bz^+ in the $C_7H_7^+$ mixture adopted by Dunbar and others is not as quantitative as hypothesized. For example, if high-internal-energy tropylium ions also react with neutral toluene, the Bz^+ fraction would appear larger than the true value, resulting in a smaller Tr^+/Bz^+ branching ratio. A third and the most likely explanation is to suppose that the internal energy estimate in the original photodissociation study was erroneous. This is all the more plausible because the internal energy content of $C_7H_8^{\bullet+}$ prior to photoabsorption was not considered at all in Dunbar's work,[3] and the experiment was carried out under the condition that the pressure and the measurement time span were not sufficient for thermalization of $C_7H_8^{\bullet+}$ generated by electron ionization. In the later and more rigorous study of the rate–energy relation,[13] a 70 times higher toluene pressure than in the earlier work was used and a 1 s time delay was allowed between the electron and laser pulses. This was to ensure the thermalization of $C_7H_8^{\bullet+}$ by collision and infrared radiative cooling. In this regard, remeasurement of the Tr^+/Bz^+ branching ratio under a more controlled condition would be useful for a better understanding of this interesting reaction system.

Conclusions

Production of $C_7H_7^+$ from $TOL^{\bullet+}$ has been investigated from the perspective of the exit channel dynamics utilizing the measured and calculated KERDs. The experimental KERDs are compatible with the well-established mechanism that the interconversion between $TOL^{\bullet+}$ and $CHT^{\bullet+}$ is rapid, and subsequent dissociations from these structures result in Bz^+ and Tr^+, respectively. The theoretical KERD in the Bz^+ channel has been calculated by the statistical phase space theory, while that in the Tr^+ channel has been obtained by the classical trajectory calculations on the PES constructed by interpolation of ab initio local potentials. Comparing these experimental and calculated KERDs, it is obvious that both Tr^+ and Bz^+ are produced as generally accepted. However, the Tr^+/Bz^+ branching ratio seems to be different from the previous reports.

This is the first time that the dissociation dynamics of a large molecular system such as $C_7H_8^{\bullet+}$ has been studied on PES constructed by interpolation of ab initio local potentials. Even though the agreement between the experimental and calculated KERDs is qualitative only, the fact that the general pattern can be reproduced by calculation is rewarding. With further development of the classical trajectory and related methods, one expects that KERD can be correctly predicted in the future.

References and Notes

(1) Lifshitz, C. *Acc. Chem. Res.* **1994**, *27*, 138.
(2) Dunbar, R. C. *J. Am. Chem. Soc.* **1973**, *95*, 472. Shen, J. S.; Dunbar, R. C.; Olah, G. A. *J. Am. Chem. Soc.* **1974**, *96*, 6227.
(3) Dunbar, R. C. *J. Am. Chem. Soc.* **1975**, *97*, 1382.
(4) Jackson, J.-A. A.; Lias, S. G.; Ausloos, P. *J. Am. Chem. Soc.* **1977**, *99*, 7515.
(5) Ausloos, P. *J. Am. Chem. Soc.* **1982**, *104*, 5259.
(6) Ohmichi, N.; Gotkis, I.; Steens, L.; Lifshitz, C. *Org. Mass Spectrom.* **1992**, *27*, 383.
(7) Lifshitz, C.; Gotkis, Y.; Ioffe, A.; Laskin, J.; Shaik, S. *Int. J. Mass Spectrom. Ion Processes* **1993**, *125*, R7.
(8) Lifshitz, C.; Gotkis, Y.; Laskin, J.; Ioffe, A.; Shaik, S. *J. Phys. Chem.* **1993**, *97*, 12291.
(9) McLafferty, F. W.; Bockhoff, F. M. *J. Am. Chem. Soc.* **1979**, *101*, 1783.
(10) Buscheck, J. M.; Ridal, J. J.; Holmes, J. L. *Org. Mass Spectrom.* **1988**, *23*, 543.
(11) Bensimon, M.; Gäumann, T.; Zhao, G. *Int. J. Mass Spectrom. Ion Processes* **1990**, *100*, 595. Zhao, G.; Gäumann, T. *Org. Mass Spectrom.* **1992**, *27*, 428.
(12) Bombach, R.; Dannacher, J.; Stadelmann, J.-P. *J. Am. Chem. Soc.* **1983**, *105*, 4205.
(13) Huang, F, –S.; Dunbar, R. C. *Int. J. Mass Spectrom. Ion Processes* **1991**, *109*, 151.
(14) Lias, S. G.; Bartmess, J. E.; Liebman, J. F.; Holmes, J. L.; Levin, R. D.; Millard, W. G. *J. Phys. Chem. Ref. Data* **1988**, Suppl. 1, 17.
(15) Lee, T. G.; Park, S. C.; Kim, M. S. *J. Chem. Phys.* **1996**, *104*, 4517.
(16) Rhee, Y. M.; Lee, T. G.; Park, S. C.; Kim, M. S. *J. Chem. Phys.* **1997**, *106*, 1003.
(17) Helgaker, T.; Uggerud, E.; Jensen, H. J. A. *Chem. Phys. Lett.* **1990**, *173*, 145. Uggerud, E.; Helgaker, T. *J. Am. Chem. Soc.* **1992**, *114*, 4265.
(18) Chesnavich W. J.; Bowers, M. T. *J. Am. Chem. Soc.* **1976**, *98*, 8301; *J. Chem. Phys.* **1977**, *66*, 2306; *Prog. React. Kinet.* **1982**, *11*, 137.
(19) Bowers, M. T.; Marshall, A. G.; McLafferty, F. W. *J. Phys. Chem.* **1996**, *100*, 12897.
(20) Hanratty, M. A.; Beauchamp, J. L.; Illies, A. J.; Koppen, P.; Bowers, M. T. *J. Am. Chem. Soc.* **1988**, *110*, 1.
(21) Baer, T. *Adv. Chem. Phys.* **1986**, *64*, 111.
(22) Aubry, C.; Holmes, J. L. *J. Phys. Chem. A* **1998**, *102*, 6441.
(23) Laskin, J.; Jimenez-Vazquez, H. A.; Shimshi, R.; Saunders: M.; de Vries, M. S.; Lifshitz, C. *Chem. Phys. Lett.* **1995**, *242*, 249.
(24) Lifshitz, C.; Levin, I.; Kababia, S.; Dunbar, R. C. *J. Phys. Chem.* **1991**, *95*, 1667.
(25) Choe, J. C.; Kim, M. S. *Int. J. Mass Spectrom. Ion Processes* **1991**, *107*, 103. Cho, Y. S.; Kim, M. S.; Choe, J. C. *Int. J. Mass Spectrom. Ion Processes* **1995**, *145*, 187.
(26) Hwang, W. G.; Moon, J. H.; Choe, J. C.; Kim, M. S. *J. Phys. Chem. A* **1998**, *102*, 7512.
(27) Oh, S. T.; Choe, J. C.; Kim, M. S. *J. Phys. Chem.* **1996**, *100*, 13367.
(28) Curtiss, L. A.; Redfern, P. C.; Smith, B. J.; Radom, L. *J. Chem. Phys.* **1996**, *104*, 5148.
(29) Curtiss, L. A.; Raghavachari, K.; Redfern, P. C.; Pople, J. A. *J. Chem. Phys.* **1997**, *106*, 1063.
(30) Frisch, M. J.; Trucks, G. W.; Schlegel, H. B.; Gill, P. M. W.; Johnson, B. G.; Robb, M. A.; Cheeseman, J. R.; Keith, T.; Petersson, G. A.; Montgomery, J. A.; Raghavachari, K.; Cioslowski, J.; Stefanov, B. B.; Nanayakkara, A.; Challacombe, M.; Peng, C. Y.; Ayala, P. Y.; Chen, W.; Wong, M. W.; Andres, J. L.; Replogle, E. S.; Gomperts, R.; Martin, R. L.; Fox, D. J.; Binkley, J. S.; Defrees, D. J.; Baker, J.; Stewart, J. P.; Head Gordeon, M.; Gonzalez, C.; Pople, J. A. *Gaussian 94*, revision E.2; Gaussian, Inc.: Pittsburgh, PA, 1995.
(31) Smith, B. J.; Hall, N. E. *Chem. Phys. Lett.* **1997**, *279*, 165.
(32) Press: W. H.; Teukolsky, S. A.; Vettering, W. T.; Flannery, B. P. *Numerical Recipes in FORTRAN*, 2nd ed.; Cambridge University Press: Cambridge, 1992.
(33) Yeh, I. C.; Kim, M. S. *Rapid Commun. Mass Spectrom.* **1992**, *6*, 115; 293.
(34) Cooks, R. G.; Beynon, J. H.; Caprioli, R. M.; Lester, G. R. *Metastable Ions*; Elsevier: New York, 1973.
(35) Matsuo, T.; Matsuda, H.; Fujita, Y.; Wollnik, H. *Mass Spectrosc.* **1976**, *24*, 19.
(36) We searched for a saddle point(s) located along the reaction path of $TOL^{\bullet+} \rightarrow Bz^+ + H^\bullet$ using various methods in ab initio packages. The attempt was fruitless. As an alternative method, we optimized the geometry with one of the CH bond lengths fixed and calculated its energy. Repeating the calculation as a function of the CH bond length, we obtained the change in the potential energy as the CH bond was lengthened. The potential energy diagrams thus obtained showed minor structures near the CH distance of 2.2–2.6 Å depending on the basis used. For example, a 0.0034 eV reverse barrier was found when the 6-31G** basis was used. This may not be a true barrier but an artifact related to the SCF error. At any rate, such barriers were too low to affect the energy partitioning significantly.
(37) Lifshitz, C. *Int. J. Mass. Spectrom. Ion Phys.* **1992**, *118/119*, 315.
(38) Park, J.; Bersohn, R.; Oref, I. *J. Chem. Phys.* **1990**, *93*, 5700.
(39) Chesnavich, W. J.; Bass, L.; Su, T.; Bowers, M. T. *J. Chem. Phys.* **1981**, *74*, 2228.
(40) Booze, J. A.; Schweinsberg, M.; Baer, T. *J. Chem. Phys.* **1993**, *99*, 4441.

(41) We have measured and calculated the KERD for $C_4H_8^{\bullet+} \rightarrow C_4H_7^+$ + H$^\bullet$. The average KERs of experimental and PST-calculated results are 74 and 68 meV, respectively. The difference between the experimental and theoretical results was not large even though a small reverse barrier ($\sim$0.1 eV) was reported (ref 39). Without proper treatment of the instrumental effect, the KERD was found to be similar to that shown in ref 38, with the average around 100 meV or larger.

(42) Unpublished results. The average KERs determined by experiment and PST calculation were 149 and 125 meV, respectively. When the instrumental broadening was not corrected for the MIKE profile obtained under the ordinary condition with a parent ion peak width of 4−5 eV, the experimental average KER of 200−260 meV was obtained.

(43) Lide, D. R., Ed. *Handbook of Chemistry and Physics*, 76th ed.; CRC: Cleveland, 1995.

(44) Lee, T. G.; Rhee, Y. M.; Kim, M. S.; Park, S. C. *Chem. Phys. Lett.* **1997**, *264*, 303.

(45) Robinson, P. J.; Holbrook, K. A. *Unimolecular reactions*; Wiley: New York, 1972.